

UC Irvine

UC Irvine Previously Published Works

Title

Radon 222 and tropospheric vertical transport

Permalink

<https://escholarship.org/uc/item/4v53t620>

Journal

Journal of Geophysical Research, 89(D5)

ISSN

0148-0227

Authors

Liu, SC
McAfee, JR
Cicerone, RJ

Publication Date

1984-08-20

DOI

10.1029/jd089id05p07291

Copyright Information

This work is made available under the terms of a Creative Commons Attribution License, available at <https://creativecommons.org/licenses/by/4.0/>

Peer reviewed

Radon 222 and Tropospheric Vertical Transport

S. C. LIU AND J. R. MCAFEE

Aeronomy Laboratory, National Oceanic and Atmospheric Administration, Boulder, Colorado

R. J. CICERONE

National Center for Atmospheric Research, Boulder, Colorado

Radon 222 is an inert gas whose loss is due only to radioactive decay with a half life of 3.83 days (5.51-day "exponential" lifetime). It is a very useful tracer of continental air because only ground level continental sources are significant. Thus it is similar in several ways to many air pollutants (e.g., NO_x (NO + NO₂), SO₂, and certain hydrocarbons). Previously published measured ²²²Rn profiles are analyzed here by averaging for the summer, winter, and spring-fall seasons. The analysis shows that in summer, about 55% of the ²²²Rn is transported above the planetary boundary layer, considerably more than during the other seasons. Similarly, in summer, about 20% rises to over 5.5 km (500 mbar). The average profiles have been used to derive vertical eddy diffusion coefficients with maximum values of $5-7 \times 10^5 \text{ cm}^2 \text{ s}^{-1}$ in the midtroposphere and 8×10^3 to $5 \times 10^4 \text{ cm}^2 \text{ s}^{-1}$ near the surface.

INTRODUCTION

Atmospheric vertical advection and turbulence play important roles in the transport of heat, momentum, moisture, and trace gases. In the long-range transport of air pollutants, vertical transport is particularly important because wind speed increases with height and heterogeneous removal and photochemical transformation of pollutants tend to be slower in the upper troposphere.

Research in turbulent transport of pollutants has concentrated on the planetary boundary layer (PBL) because of interest in urban air quality [e.g., *Demerjian*, 1976; *Turner*, 1979]. This is the case even for most of the so-called long-range transport (≥ 1000 km) models (see reviews by *Bass* [1980] and *Dittenhoefer* [1982]). Recently, some attempt [e.g., *Lamb*, 1983] has been made to deal with the transport of pollutants between the PBL and the free troposphere.

On the other hand, global tropospheric tracer models employ various parameterizations to simulate vertical transport. In the one- or two-dimensional models, vertical eddy diffusion coefficients are used with values usually in the range $1-3 \times 10^5 \text{ cm}^2 \text{ s}^{-1}$ [e.g., *Chameides and Stedman*, 1977; *Thompson and Cicerone*, 1982]. Such eddy coefficients were derived from a few measured tropospheric profiles of tracers such as ²²²Rn, ²¹⁰Pb, and ¹⁴CO₂ (see, for example, *Machta* [1974], *Johnston et al.* [1976], *Businger et al.* [1971], *Jacobi and Andre* [1963], and *Beck and Gogolak* [1979]). Three-dimensional general circulation models calculate resolvable large-scale advection wind velocities while parameterizing the unresolvable transport such as turbulence and convective activities associated with cumulus clouds.

Recently, *Gidel* [1983] and *Chatfield and Crutzen* [1984] have made one-dimensional parameterizations of the vertical transport of trace species due to cumulus clouds and found it to be highly efficient. Because of deep convective activities, an increasing mixing ratio with height in the troposphere can exist for some short-lived gases with only a surface source [*Chatfield*, 1982; *Gidel*, 1983].

Radon 222 and its decay daughters have frequently been used as tracers for studying vertical diffusivity because of its well-defined source and sink. Radon 222 is a radioactive noble gas in the decay series of ²³⁸U. The source of ²²²Rn is trace amounts of ²³⁸U present in all soils in varying amounts. Being an inert gas with relatively small solubility, ²²²Rn may be released to pore space between soil particles and diffuse into the atmosphere. The only significant sink of atmospheric ²²²Rn is radioactive decay with a half life of 3.83 days, which corresponds to an exponential decay "lifetime" of 5.51 days. The turbulent diffusion coefficient $K(z, t)$ as a function of the height z above the ground and the time t has been derived by many workers [*Jacobi and Andre*, 1963; *Malakhov et al.*, 1966; *Israel et al.*, 1966; *Ikebe*, 1970; *Roffman*, 1972; *Li*, 1975; *Beck and Gogolak*, 1979]. However, these studies were either limited to a few specific measurements of ²²²Rn and its decay daughters or limited only to transport within the PBL. On the other hand, eddy diffusion coefficients derived from excess ¹⁴CO₂ do not have enough vertical resolution in the troposphere [*Davidson et al.*, 1966; *Seitz et al.*, 1968].

In this paper we try to compile a statistically more meaningful average vertical profile of ²²²Rn measured in the troposphere. Special emphasis will be given to the ²²²Rn distribution in the summer in order to test various models and parameterizations of the vertical transport associated with cumulus clouds. A corresponding eddy coefficient will be derived from the average ²²²Rn profile.

The lifetime and source characteristics (i.e., emitted at the surface) of ²²²Rn are of the same order as many air pollutants such as NO_x (NO + NO₂), propane, butane, and other moderately reactive hydrocarbons. We will discuss the implications of applying the derived eddy coefficients to trace gases with various lifetimes.

COMPILATION OF MEASURED ²²²RN PROFILES

We have made a literature search of measured vertical profiles of ²²²Rn. Since our primary interest is to characterize the vertical transport from the surface to the tropopause, profiles that do not reach beyond the top of the PBL are excluded in this paper. These data, mostly taken from meteorological towers, will be addressed in a future study. Measurements made over the ocean are also excluded because of a scarcity of

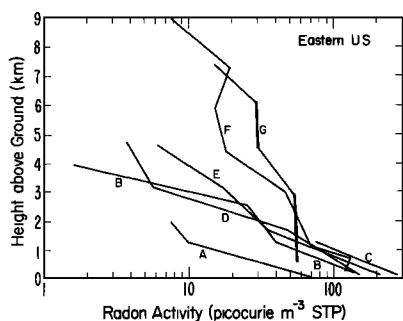


Fig. 1. Measured ^{222}Rn profiles over the eastern United States. Profiles A–E are from central Illinois in 1967 [Bradley and Pearson, 1970]: A, July 14; B, July 26; C, August 3; D, September 6; E, September 20. Profiles F and G are from Ohio in 1950 [Wexler et al., 1956]: F, October 25; G, October 26.

data. Most of the ^{222}Rn in the maritime air is advected from continents and is deposited over oceans as ^{210}Pb . Measurements of ^{222}Rn and ^{210}Pb in the maritime air will be valuable for studying transport processes over oceans [Kritz, 1983].

The published profiles of ^{222}Rn made over continental land masses are shown in Figures 1–5. The activity, converted to a standard of picocuries per cubic meter (STP) where necessary, is proportional to the mixing ratio of ^{222}Rn and is plotted as a function of height above ground rather than above sea level.

Two sets of measurements from the eastern United States are shown in Figure 1, both inferred from radon daughter measurements. The curves labeled F and G are two very early profiles from October 1950 in Ohio [Wexler et al., 1956]. These measurements are arbitrarily normalized, since the absolute values are uncertain and neither time of day nor weather conditions are given. They show a day-to-day variation and an effective vertical mixing. In contrast, the results from Illinois [Bradley and Pearson, 1970] during July through September 1967 (curves A–E) demonstrate considerably less mixing. This may be a consequence of the sampling period between local 0900 and 1300. Curves B–E are very consistent, particularly in the 0- to 2-km region, despite the 2-month interval and differing weather, namely, clear, in a cumulus squall line, stagnant clear high pressure, and in fair weather cumulus, respectively. The counting error is about 3–5 pCi m^{-3} . The authors explain the extremely low case, curve A, as being due to an Arctic air mass.

Results from the European Soviet Union are shown in

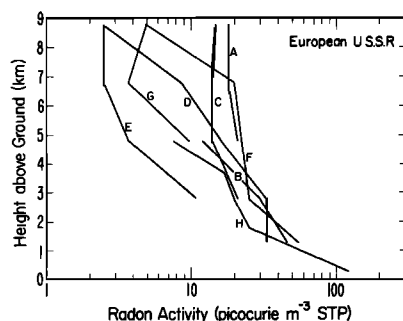


Fig. 2. Measured ^{222}Rn profiles from the Soviet Union. Profiles A–G are from European USSR [Nazarov et al., 1970]: A–E, eastern Ukraine, July 7, 22, 24, 27, and 28, 1966, respectively; F and G near Moscow, January and February 1967. Profile H is from Central Asia, October 15, 1958 [Kirichenko, 1962].

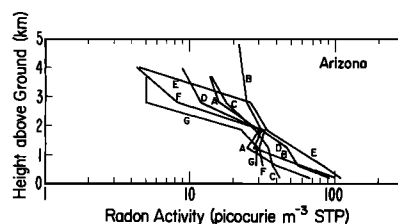


Fig. 3. Measured ^{222}Rn profiles from Arizona in the SW United States during summer 1971 [Larson and Hoppel, 1973]. Profiles A–G refer to August 24, 25, 26, 28, 29, 30, and 31, respectively.

Figure 2, again inferred from daughters. There is a large amount of variation in curves A–G [Nazarov et al., 1970], but no measurement accuracies or times of day were given. Curves A–E are July, eastern Ukraine measurements, while curves F and G are from near Moscow in January and February. Any seasonal variation is hidden in the short-term variability, which is apparent for both summer and winter in the well-mixed examples (curves A, C, and F) and the poorly mixed examples (curves B, D, E, and G). This may be a consequence of the time of day of the measurements. An additional set of measurements [Kirichenko, 1962] is shown as curve H, an October measurement in central Asia. Again, neither measurement accuracies nor time of day were given, but the atmosphere was stably stratified.

A set of profiles [Larson and Hoppel, 1973] from SW Arizona in late August 1971 are shown in Figure 3. The morning-to-midday period is represented by curves A–E, late evening by curve F, and afternoon by curve G, but all are within a 1-week period. The large day-to-day variation is clearly evident, as is the dividing feature just below 2 km. According to these authors the diurnal variation is not important above the 2-km break. The 95% confidence level in the counting statistics is about 5 pCi m^{-3} , and radon is inferred from the daughter measurements.

A similar set of profiles [Larson, 1974] were made over the Yukon Valley of Alaska during February 1972 and are shown in Figure 4. The standard deviation in counting ranges from 1 to 5 pCi m^{-3} and times of day are not given. Conditions for curves A–C were dominated by a high-pressure system with a low-level inversion, while curve D represented a new air mass advected into the area. Throughout the measurement period a snow cover of 58.4 cm persisted, and the author used the large radon concentration near the surface to argue that emanation is not severely inhibited by frost and snow cover.

Results from the western United States with radon measured directly are shown in Figure 5. Curves A–F [Moore et al., 1973] represent measurements at three locations and

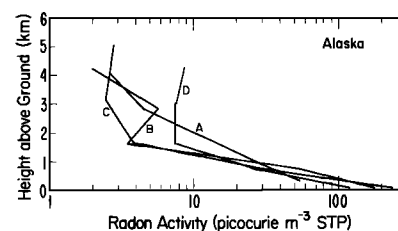


Fig. 4. Measured ^{222}Rn profiles from the Yukon Valley of Alaska during winter 1972 [Larson, 1974]. Profiles A–D refer to February 15, 20, 21, and 22, respectively.

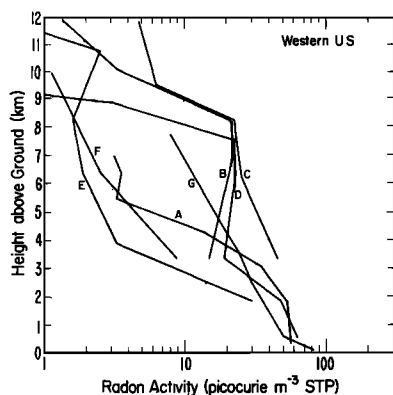


Fig. 5. Measured ^{222}Rn profiles from the western United States. Profiles A–F are from three locations over a 3-year period [Moore et al., 1973]: A, April 2, 1969, Limon, Colorado; B and C, May 18 and August 18, 1971, Scottsbluff, Nebraska; D, August 31, 1971, Salt Lake City, Utah; and E and F, November 12, 1971, and January 25, 1972, Scottsbluff, Nebraska. Profile G is an average of six profiles in the summer of 1968 in the Rio Grande Valley of New Mexico [Wilkening, 1970].

throughout the year. One-sigma counting errors are $1.48 \pm 0.74\%$ of the measured values. Basically, curves B–D are warm weather, and curves A, E, and F are cold weather. The difference by season is very evident in the 4- to 8-km region. Also noticeable in these measurements is the behavior at the tropopause. Examples where penetration of the measured tropopause occurred are curve B at a height of about 8.2 km (above ground level) and curve F at a height of about 10 km. Times of day and weather conditions are not given. Also shown in Figure 5 are results from the Rio Grande Valley in New Mexico [Wilkening, 1970] as represented by curve G, an average of six profiles obtained over the course of a single day under fair weather conditions. The random counting error is approximately 15%. The morning flights are characterized by high ^{222}Rn concentrations in the boundary layer. In the afternoon flights the boundary layer values are depleted by a factor of 5 or more because of convective mixing.

Because of the expected variation in vertical mixing with season, the profiles in Figures 1–5 have been divided into three groups: summer (June, July, and August (23 profiles)); spring and fall (March, April, May, September, October, and November (eight profiles)); and winter (December, January, and February (seven profiles)). Average values for all three of the seasonal divisions are shown in Figure 6. The New Mexico data are included in the summer curve with a sixfold weighting. The standard deviation averaged over every 2 km is denoted by a bar for the summer profile. The largest standard deviation for the summer profile is $\pm 76\%$ near 4 km, while the spring–fall and winter values are not plotted because of the smaller number of profiles. No standard deviation is given at the surface or 12 km because of lack of data. The discontinuities in the profiles are a result of the appearance and disappearance of individual profile contributions due to their respective altitude measurement ranges. For instance, the discontinuity near 4 km for the summer average is caused by the disappearance of the Arizona profiles and one of the Illinois profiles. Since these profiles generally have small values at the top of their measuring range, the average above this point increases when they no longer contribute. Such discrepancies are clearly nonphysical and are present only because the individual measured profiles do not cover the entire troposphere.

DISCUSSION

The average summertime ^{222}Rn mixing ratio profile shows the least decrease with height compared to the other two seasons. This is consistent with the generally accepted fact that vertical mixing is more efficient in the warmer season because of the solar heating–induced mixing. The difference between the summer profile and the other two profiles should not be regarded as quantitative, because of the sparseness of data in nonsummer seasons, as discussed above.

The slope of the summer profile has some interesting features. It starts relatively steeply below 3 km and gradually levels off between 3 and 8 km. Above that the influence of the stable tropopause starts to become important. The locations of the tropopause in this figure are not well defined because individual tropopause altitudes, where given, range from about 9 to 16 km. Most of the measurements did not reach above the tropopause.

Because of poor height resolution, it is difficult to identify mechanisms that contribute to the steep slope below 3 km. The slow exchange between the PBL and the overlying free troposphere must contribute in part [Wilkening, 1970]. Since the top of the PBL usually increases during the daytime [Kaimal et al., 1976] and the ^{222}Rn measurements were made at various daytime hours, the average profile of ^{222}Rn below 2 km should not be considered to represent daytime turbulent diffusion within the PBL, which is known to be fast [e.g., Kaimal et al., 1976]. It should only be regarded as representing the effective mixing that includes both daytime and nighttime atmospheric processes. On the other hand, since none of these data were taken at night, the average profile definitely has a daytime bias. This bias significantly affects the ^{222}Rn distribution in the PBL; above it the effect is probably small.

Between 3 and 8 km the summer ^{222}Rn mixing ratio decreases by about 60%, in comparison to an 80% decrease between the surface and 3 km. Clearly, efficient vertical transport in the 3- to 8-km region is required. The vertical transport can be either by advection or by turbulence, or both. In fact, below 8 km the profile, to a certain extent, resembles the tracer profile calculated by the advective cumulus cloud model of Gidel [1983]. In that model, Gidel assumed a surface source and a lifetime of 4 days for an NO_x -like tracer. Except for the slightly shorter lifetime, this tracer is identical to ^{222}Rn . In

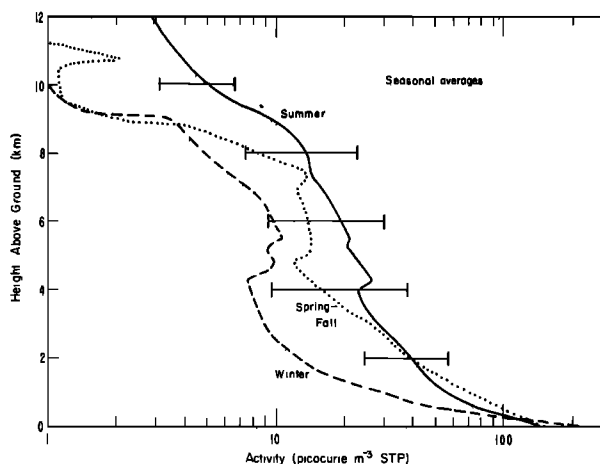


Fig. 6. Average ^{222}Rn profiles for the three seasonal divisions: summer, spring and fall, and winter. The error bars represent one standard deviation for the summer case.

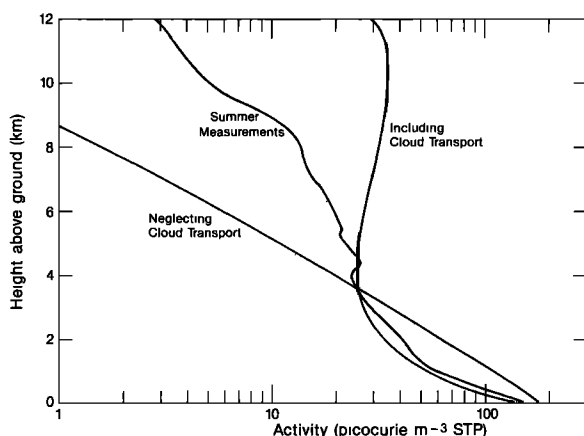


Fig. 7. Model profiles of a gas with surface source and a 4-day lifetime with and without cloud transport [Gidel, 1983]. The average summer profile of Figure 6 is included for comparison (arbitrary units).

Figure 7, two model-calculated profiles of Gidel [1983] are compared to the average summer ^{222}Rn profile. The calculated profiles have been shifted linearly by arbitrary factors to facilitate comparison. The two represent the previously mentioned advective cumulus model and a cloudless transport model. The summer ^{222}Rn profile is in reasonable agreement with either model in the region below 3 km. Between 3 and 8 km the measurements show a much greater effective vertical mixing than the cloudless model and much less than the cloud-included model. If the difference in lifetime is taken into account, the measurements would be closer to the cloudless model, but farther from the advective cumulus model. Part of the discrepancy is due to the fact that the model calculations are parameterized for the tropical troposphere [Gidel, 1983], and part may also be due to horizontal transport, as discussed below.

The change of slope and the increasing mixing ratio with height in the model-calculated tracer profile are the result of advective activities associated with cumulus cloud which draws in air (and trace species) near the surface, pulls upward in the updraft, and releases it near the cloud top [Gidel, 1983; Chatfield and Crutzen, 1984]. Although the vertical transport due to this mechanism is quite strong, only a small percentage of the earth's surface is covered by active updrafts at any time. Modeling the overall effect by the updraft is obviously subject to large uncertainty.

The observations for the winter and spring-fall seasons show both similarities to and differences from the summer profile. In the spring-fall case, the low-altitude gradient is similar but extends upward to 5 km. In the winter case, the slope is much greater below 2 km, with a smaller but similar transport above. However, there are insufficient observations in the winter and in the spring and fall to give climatologically meaningful averages. The seasonal difference shown here should be regarded only as qualitative.

An important question is to determine the representativeness of the average summer ^{222}Rn profile. One way to test this is to compare the derived surface ^{222}Rn flux from the average profile to values measured directly that range from 0.25 to 2 atoms $\text{cm}^{-2} \text{s}^{-1}$, with an average value near 0.75 [Wilkening et al., 1975; Turekian et al., 1977]. To derive the surface flux from the average profile, one needs to include two components: the column radioactive loss of ^{222}Rn and

the flux divergence. Estimating the first term is straightforward. The total column abundance is about 20 pCi cm^{-2} ($3.5 \times 10^5 \text{ atoms cm}^{-2}$), which implies an average column loss of $4.2 \times 10^{-17} \text{ Ci cm}^{-2} \text{ s}^{-1}$ ($0.74 \text{ atom cm}^{-2} \text{ s}^{-1}$). In theory the second term could be evaluated by calculating the trajectory for individual ^{222}Rn measurement. This is not practical because the back trajectory of each air mass would have to be analyzed for more than 5 days (^{222}Rn lifetime). However, trajectory analyses for a few selected profiles may be useful to study the effect of long-range transport on the ^{222}Rn distribution. A rough estimate can be obtained by calculating the divergence over the continental United States. The ^{222}Rn flux through the tropopause is negligible in comparison to horizontal divergence. The horizontal divergence is approximately equal to the ^{222}Rn profile multiplied by the summer average zonal wind velocity. We have used the zonal wind data compiled by Oort and Rasmussen [1971]. The resultant ^{222}Rn horizontal divergence (or flux to the ocean) is about 50% of the column decay rate, i.e., $0.37 \text{ atom cm}^{-2} \text{ s}^{-1}$. Thus the surface flux deduced from the summer ^{222}Rn vertical profile is about 1.1 atoms $\text{cm}^{-2} \text{ s}^{-1}$, about 50% higher than the average flux measured directly. Qualitatively, this is consistent with the fact that the ^{222}Rn flux is higher in warmer seasons as discussed above. In addition, Turekian et al. [1977] argued that the actual average continental ^{222}Rn surface flux should be about 1.2 atoms $\text{cm}^{-2} \text{ s}^{-1}$, in excellent agreement with our estimate. The agreement implies that the average summer ^{222}Rn profile gives a representative surface flux. This can be used to argue that the summer ^{222}Rn profile below 4 km, from which most of the ^{222}Rn flux is derived, is representative of the real continental ^{222}Rn distribution. However, it does not provide any test on the representativeness of the ^{222}Rn distribution above 4 km.

In view of the large standard deviation and lack of other independent methods to test the representativeness of the average ^{222}Rn profiles compiled here, they cannot be claimed to be statistically meaningful. However, these profiles are by far the most extensive data compiled for a tropospheric tracer with simple chemistry. In the following section, we will assume that the ^{222}Rn profiles are representative of the average distributions over the continents and can be used to derive vertical eddy coefficients.

CALCULATION OF ONE-DIMENSIONAL EDDY COEFFICIENT

The continuity equation for ^{222}Rn can be written as

$$\frac{\partial n}{\partial t} = \frac{\partial}{\partial z} \left[K_z N \frac{\partial (n/N)}{\partial z} \right] - \lambda n - u_z \frac{\partial n}{\partial x} \quad (1)$$

where n represents the ^{222}Rn density; N is the background density, which is a function of altitude; K_z is the vertical eddy coefficient; and λ is the radioactive decay constant (inverse of exponential lifetime). This kind of expression has been traditionally used in the one-dimensional stratospheric and tropospheric photochemical models [cf. Johnston et al., 1976; Thompson and Cicerone, 1982]. In a more rigorous treatment of vertical transport the advection or mean wind term should be separated from turbulent motion, and only the latter would be parameterized by an eddy coefficient [cf. Mahman, 1976; Gidel, 1983].

Nevertheless, a single overall vertical eddy coefficient has been used profitably in one-dimensional modeling of various stratospheric and tropospheric tracer distributions. The back-

ground density at various heights is taken from the spring-fall model of U.S. Standard Atmosphere, Supplement (1966). The last term in (1) is due to zonal transport of ^{222}Rn , where u_z denotes the mean zonal wind velocity and x is the longitude. To calculate this term, we assume the average summer profile to be the average steady state profile over the United States. Since there is negligible transport of ^{222}Rn from the ocean to the continent, the last term can be approximated by the transport of continental ^{222}Rn to the ocean, i.e., $u_z n/l$, where $l \approx 5000$ km is the longitudinal width of the U.S. continent.

With many discontinuities in the ^{222}Rn profiles that are artifacts due to data averaging, a negative or unreasonable eddy coefficient may result. Without an objective method to smooth the ^{222}Rn profiles, we elect to solve (1) as follows. Equation (1) was solved only over those portions of the average profiles having a continuous set of contributing individual profiles, thus avoiding the problem of the discontinuities. Interpolation then provided values in the remaining portions, where individual profiles were beginning or ending. The results are shown in Figure 8. For the summer case the eddy coefficient K_z increases rapidly from 5×10^4 $\text{cm}^2 \text{s}^{-1}$ at ground level to values near 7×10^5 between 4 and 8 km and decreases to 6×10^4 at 12 km. The smaller eddy diffusion coefficient in the PBL reflects the influence of the nocturnal inversion layer in the summer that inhibits vertical transport at night. In winter, with frequent inversions even in the daytime, the vertical transport near the surface is more than a factor of 5 slower than that in the summer. Increase of vertical transport with height in the midtroposphere is expected because of stronger zonal flows and the lack of inversion layers. In the upper troposphere the vertical transport decreases significantly because of the stabilizing effect of the tropopause and stratosphere. This is consistent with the eddy coefficient of about $2\text{--}4 \times 10^3$ $\text{cm}^2 \text{s}^{-1}$ in the lower stratosphere derived from stratospheric tracers such as CH_4 and $^{14}\text{CO}_2$ (see, for example, Johnston *et al.* [1976]).

The eddy coefficients for the other two seasons show the same general behavior as for the summer case, but with generally lower values, as expected. The detailed behavior is even more suspect because of the smaller number of data. Inclusion of the last term of (1) (i.e., horizontal divergence) increases the calculated eddy coefficient significantly in comparison to the eddy diffusion coefficient calculated without the term.

To evaluate the vertical transport of air pollutants, such as

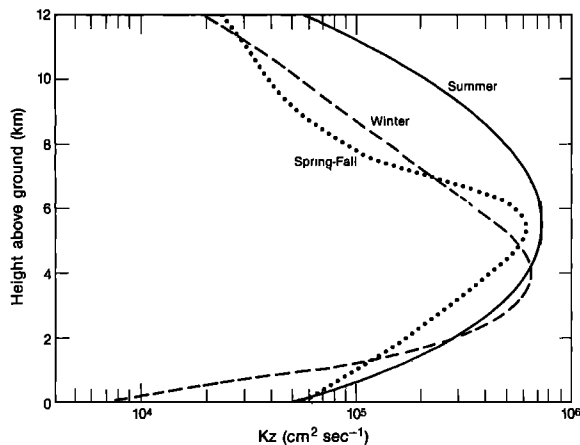


Fig. 8. Vertical eddy diffusion coefficients K_z derived from the profiles of Figure 6. By contrast, most one-dimensional models use values near 10^5 $\text{cm}^2 \text{s}^{-1}$ throughout the troposphere.

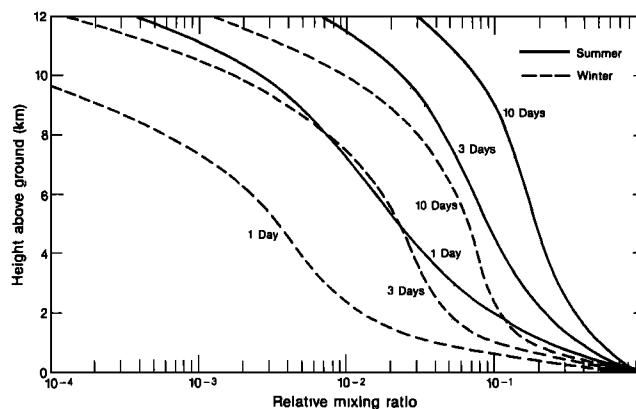


Fig. 9. Calculated summer and winter profiles of trace gases with assumed lifetimes of 1, 3, and 10 days.

NO_x , SO_2 , and hydrocarbons, we have made model calculations for tracer gases with lifetimes of 1, 3, and 10 days that encompass the lifetimes of most pollutants. Equation (1) is now solved for n by using the summer and winter eddy diffusion coefficients. The trace gases are assumed to be released at the surface with surface mixing ratios normalized to an arbitrary unit of 1. The results are shown in Figure 9. The summer profiles are given by the solid curves. If we assume that the top of the boundary layer in the summer is at 2 km, the fractions of trace gases transported above the boundary layer are about 20, 40, and 70% for trace gas lifetimes of 1, 3, and 10 days, respectively. These values include the portions transported to the oceans which are 1, 6, and 25% of the total emissions for the trace gases with the three lifetimes, respectively. For ^{222}Rn the amount transported above 2 km is 55%, and the amount transported to the ocean is 13% of the surface emission. In the winter, much less is transported to the same height. However, if we assume the top of the boundary layer is at 1 km in the winter, similar amounts would reach above the boundary layer and be transported to the ocean. One should use these estimates with caution, since the removal process of the trace gas is assumed here to be independent of atmospheric motion. This is obviously not true for many soluble atmospheric gases, such as SO_2 and HNO_3 , that are removed by heterogeneous processes closely related to atmospheric motions. For instance, condensation and precipitation tend to occur frequently in the ascending air but not descending air.

COMPARISON WITH PREVIOUSLY DERIVED EDDY COEFFICIENTS

As is discussed in previous sections, eddy coefficients derived previously from observed ^{222}Rn profiles were based on only one or a few limited measurements [e.g., Jacobi and Andre, 1963]. The two profiles used by Jacobi and Andre consist of a subset of the average profile for spring and fall in Figure 7. However, as is discussed above, these spring-fall eddy coefficients are not meaningful because of lack of data.

Bolin and Bischof [1970] measured vertical profiles and seasonal variations of CO_2 in the latitude band of about $50^\circ\text{--}70^\circ\text{N}$, mostly over Scandinavia. The seasonal variations with amplitude decreasing with height and a small phase lag are due to biological activities. Bolin and Bischof deduced a vertical diffusion coefficient from both the amplitude decrease and the phase lag. They obtained a coefficient of 1.4×10^5 $\text{cm}^2 \text{s}^{-1}$ between 2 and 10 km. However, as was noticed by

Machta [1974], Bolin and Bischof assumed a constant density with height. Using the standard atmosphere, Machta [1974] deduced an appreciably smaller eddy coefficient, $5 \times 10^4 \text{ cm}^2 \text{ s}^{-1}$, from Bolin and Bischof's CO_2 data. This value should be regarded as an annual average vertical eddy coefficient between 2 and 10 km in the latitude band of about $50^\circ\text{--}70^\circ\text{N}$. Averaging our eddy coefficients between 2 and 10 km gives a value that is about 6 times that of Bolin and Bischof's. Part of the difference is probably due to the fact that most ^{222}Rn data were taken at lower latitudes, where convective activities are stronger than at $50^\circ\text{--}70^\circ\text{N}$.

In the analysis of vertical distributions of Aitken particles from several flights, Junge [1963] estimated that the average eddy coefficient is in the range of 10^5 to $5 \times 10^5 \text{ cm}^2 \text{ s}^{-1}$, which is qualitatively consistent with our values.

The eddy coefficients derived from excess $^{14}\text{CO}_2$ usually show a smaller value of about 10^4 to $10^5 \text{ cm}^2 \text{ s}^{-1}$ [Davidson et al., 1966; Seitz et al., 1968]. Excess $^{14}\text{CO}_2$ was injected into the stratosphere by nuclear bomb tests, mostly in the early 1960's. It is transported slowly into the troposphere and is eventually assimilated by the biosphere and dissolved in the ocean. The excess $^{14}\text{CO}_2$ is a different tracer from ^{222}Rn , Aitken particles, and CO_2 , because it is transported downward from the stratosphere. Its vertical distribution is affected differently from upward moving tracers when advective motion is important.

CONCLUSIONS

We have compiled 38 measurements of tropospheric ^{222}Rn vertical distribution. Although these data may not be representative of the average tropospheric profile, the extensive data, especially in the summer, warrant an examination of the vertical transport in the troposphere. Upward mixing in the midtroposphere is efficient, but not nearly as much as predicted by cumulus cloud transport models. Eddy diffusion coefficients deduced from the average ^{222}Rn data show low values near ground level, larger values in the midtroposphere, and a decrease as the tropopause is approached. For a pollutant with a lifetime similar to ^{222}Rn and a surface source, at least 50% would reach the free troposphere above the PBL in the summer, less during the rest of the year. Additional measurements, with more vertical resolution and extended coverage from the ground to the tropopause over lands and oceans, are desirable from the standpoint of providing more detailed and accurate parameterizations of tropospheric vertical transport. Because there is a net transport of ^{222}Rn to the oceans and also vertical wind shear, it is desirable to calculate the ^{222}Rn distribution in a three-dimensional model.

Acknowledgments. We appreciate the discussions with R. Chatfield, D. Lenschow, J. Mahlman, and J. Wyngaard. The comments of three reviewers are very helpful and appreciated. This work was conducted as part of the National Acid Precitation Assessment Program and was funded by the National Oceanic and Atmospheric Administration. The National Center for Atmospheric Research is sponsored by the National Science Foundation.

REFERENCES

- Bass, A., Modeling long range transport and diffusion, *Jt. Conf. Appl. Air Pollut. Meteorol. Conf. Pap.*, 2nd, 193, 1980.
- Beck, H. L., and C. V. Gogolak, Time-dependent calculations of the vertical distribution of ^{222}Rn and its decay products in the atmosphere, *J. Geophys. Res.*, 84, 3139, 1979.
- Bolin, B., and W. Bischof, Variations of the carbon dioxide content of the atmosphere in the northern hemisphere, *Tellus*, 22, 431, 1970.
- Bradley, W. E., and J. E. Pearson, Aircraft measurements of the vertical distribution of radon in the lower atmosphere, *J. Geophys. Res.*, 75, 5890, 1970.
- Businger, J. A., J. C. Wyngaard, Y. Izumi, and E. F. Bradley, Flux-profile relationships in the atmospheric surface layer, *J. Atmos. Sci.*, 28, 181, 1971.
- Chameides, W. L., and D. H. Stedman, Tropospheric ozone: Coupling transport and photochemistry, *J. Geophys. Res.*, 82, 1787, 1977.
- Chatfield, R. B., Remote tropospheric SO_2 : Cloud transport of reactive sulfur emissions, *Coop. Thesis 70*, Natl. Center for Atmos. Res., Boulder, Colo., 1982.
- Chatfield, R. B., and P. J. Crutzen, Sulfur dioxide in remote oceanic air: Cloud transport of reactive precursors, *J. Geophys. Res.*, this issue, 1984.
- Davidson, B., J. P. Friend, and H. Seitz, Numerical models of diffusion and rainout of stratospheric radioactive materials, *Tellus*, 18, 301, 1966.
- Demerjian, K. L., Photochemical diffusion models for air quality simulation: Current status. Assessing transportation-related impacts, *Spec. Rep. 167*, pp. 21–23, Trans. Res. Board, Natl. Acad. of Sci., Washington, D. C., 1976.
- Dittenhoefer, A. C., A critical review of P.M. long range transport/acid precipitation models, paper presented at 75th Annual Meeting, Air Pollut. Control Assoc., New Orleans, La., June 20–25, 1982.
- Gidel, L. T., Cumulus cloud transport of transient tracers, *J. Geophys. Res.*, 88, 6587, 1983.
- Ikebe, Y., Variations of radon and thoron concentrations in relation to wind speed, *J. Meteorol. Soc. Jpn.*, 48, 461, 1970.
- Israel, H., M. Hobert, and G. W. Israel, Results of continuous measurements of radon and its decay products in the lower atmosphere, *Tellus*, 18, 638, 1966.
- Jacobi, W., and K. Andre, The vertical distribution of radon 222, radon 220, and their decay products in the atmosphere, *J. Geophys. Res.*, 68, 3799, 1963.
- Johnston, H. S., D. Kattenhorn, and G. Whitten, Use of excess carbon 14 data to calibrate models of stratospheric ozone depletion by supersonic transports, *J. Geophys. Res.*, 81, 368, 1976.
- Junge, C. E., *Air Chemistry and Radioactivity*, Academic, New York, 1963.
- Kaimal, J. C., J. C. Wyngaard, P. A. Haugen, O. R. Cote, Y. Izumi, S. J. Caughey, and C. J. Readings, Turbulence structure in the convective boundary layer, *J. Atmos. Sci.*, 33, 2152, 1976.
- Kirichenko, L. V., The vertical distribution of the products of decay of radon in the free atmosphere, in *Problems of Nuclear Meteorology*, edited by I. L. Karol and S. G. Malakhov, pp. 99–124, State Publishing House for Literature in the Field of Atomic Science and Engineering, Moscow, 1962.
- Kritz, M. A., Use of long-lived radon daughters as indicators of exchange between the free troposphere and the marine boundary layer, *J. Geophys. Res.*, 88, 8569, 1983.
- Lamb, R. G., A regional scale (1000 km) model of photochemical air pollution, I, Theoretical formulation, report, U.S. Environ. Prot. Agency, Research Triangle Park, N.C., 1983.
- Larson, R. E., Radon profiles over Kilauea, the Hawaiian Islands and Yukon Valley snow cover, *Pure Appl. Geophys.*, 112, 204, 1974.
- Larson, R. E., and W. A. Hoppel, Radon 222 measurements below 4 km as related to atmospheric convection, *Pure Appl. Geophys.*, 105, 900, 1973.
- Li, T., Prediction of the diurnal variation of radon diffusion with synoptic implications, *Arch. Meteorol. Geophys. Bioklimatol.*, Ser. A, 24, 269, 1975.
- Machta, L., Global scale atmospheric mixing, *Adv. Geophys.*, 18B, 33, 1974.
- Mahlman, J. D., Some fundamental limitations of simplified transport models as implied by results from a three-dimensional general-circulation/tracer model, *Proc. Conf. Clim. Impact Assess. Program*, 4th, 1975, 132, 1976.
- Malakhov, S. G., V. N. Bakulin, G. V. Dimitrieva, L. V. Kirichenko, T. I. Sisigina, and B. G. Starikov, Diurnal variations of radon and thoron decay product concentrations in the surface layer of the atmosphere and their washout by precipitations, *Tellus*, 18, 643, 1966.
- Moore, H. E., S. E. Poet, and E. A. Martell, ^{222}Rn , ^{210}Pb , ^{210}Bi , and ^{210}Po profiles and aerosol residence times versus attitude, *J. Geophys. Res.*, 78, 7065, 1973.
- Nazarov, L. E., A. F. Kuzenkov, S. G. Malakhov, L. A. Volokitina, Ya. I. Gaziyevev, and A. S. Vasil'yev, Radioactive aerosol distribution

- in the middle and upper troposphere over the USSR in 1963–1968, *J. Geophys. Res.*, **75**, 3575, 1970.
- Oort, A. H., and E. M. Rasmussen, Atmospheric circulation statistics, *NOAA Prof. Pap. 5*, U.S. Dept. of Commer., Rockville, Md., Sept. 1971.
- Roffman, A., Short-lived daughter ions of radon 222 in relation to some atmospheric processes, *J. Geophys. Res.*, **77**, 5883, 1972.
- Seitz, H., B. Davidson, J. P. Friend, and H. W. Feely, Final report on project streak. Numerical models of transport, diffusion and fall-out of stratospheric radioactive material, *USAEC Rep. NYO-3654-4*, 97 pp., Isotopes, Inc., Westwood, N. J., 1968.
- Thompson, A. M., and R. J. Cicerone, Clouds and wet removal as causes of variability in the trace-gas composition of the marine troposphere, *J. Geophys. Res.*, **87**, 8811, 1982.
- Turekian, K. K., Y. Nozaki, and L. K. Benninger, Geochemistry of atmospheric radon and radon products, *Annu. Rev. Earth Planet. Sci.*, **5**, 227, 1977.
- Turner, D. B., Atmospheric dispersion modelling: A critical review, *J. Air Pollut. Control Assoc.*, **29**, 502, 1979.
- Wexler, H., L. Machta, D. H. Pack, and F. D. White, Atomic energy and meteorology, *Proc. Int. Conf. Peaceful Uses At. Energy, Ist.*, **1955**, **13**, 333, 1956.
- Wilkening, M. H., Radon 222 concentrations in the convective patterns of a mountain environment, *J. Geophys. Res.*, **75**, 1733, 1970.
- Wilkening, M. H., W. E. Clements, and D. Stanley, Radon-222 flux measurements in widely separated regions, The Natural Radiation Environment, II, *Rep. USERDA CONF-720805*, edited by J. A. S. Adams, pp. 717–730, U.S. Energy Res. and Dev. Admin., Washington, D. C., 1975.
- R. J. Cicerone, National Center for Atmospheric Research, P.O. Box 3000, Boulder, CO 80307.
- S. C. Liu and J. R. McAfee, Aeronomy Laboratory, National Oceanic and Atmospheric Administration, 325 Broadway, Boulder, CO 80303.

(Received November 29, 1983;
revised April 26, 1984;
accepted April 30, 1984.)